
Semantic Volume: Quantifying and Detecting both External and Internal Uncertainty in LLMs

Xiaomin Li*
Harvard University

Zhou Yu
Amazon

Ziji Zhang
Amazon

Yingying Zhuang
Amazon

Swair Shah
Amazon

Anurag Beniwal
Amazon

Abstract

Large language models (LLMs) have demonstrated remarkable performance across diverse tasks by encoding vast amounts of factual knowledge. However, they are still prone to hallucinations, generating incorrect or misleading information, often accompanied by high uncertainty. Existing methods for hallucination detection primarily focus on quantifying *internal uncertainty*, which arises from missing or conflicting knowledge within the model. However, hallucinations can also stem from *external uncertainty*, where ambiguous user queries lead to multiple possible interpretations. In this work, we introduce *Semantic Volume*, a novel mathematical measure for quantifying both external and internal uncertainty in LLMs. Our approach perturbs queries and responses, embeds them in a semantic space, and computes the determinant of the Gram matrix of the embedding vectors, capturing their dispersion as a measure of uncertainty. Our framework provides a generalizable and unsupervised uncertainty detection method without requiring internal access to LLMs. We conduct extensive experiments on both external and internal uncertainty detection, demonstrating that our Semantic Volume method consistently outperforms existing baselines in both tasks. Additionally, we provide theoretical insights linking our measure to differential entropy, unifying and extending previous sampling-based uncertainty measures such as the semantic entropy. Semantic Volume is shown to be a robust and interpretable approach to improving the reliability of LLMs by systematically detecting uncertainty in both user queries and model responses.

1 Introduction

Large language models encode extensive knowledge from massive training data and have shown remarkable achievements on diverse tasks [10, 1, 41, 3, 6, 18, 5]. Despite their success, LLMs still exhibit hallucination: generating information or conclusions that are incorrect, incomplete, fabricated, or misleading [21, 20, 8, 17, 11, 9]. These hallucinations can propagate false information, undermine decision-making, and damage the credibility of AI systems. Detecting the hallucination is a challenging task, and a growing stream of research leverages the uncertainty in LLMs for hallucination detection [27, 14, 13, 23, 35, 15, 25, 32, 33, 38]. Existing methods focus on **internal uncertainty**, which generally arises from missing relevant knowledge, conflicting information, or outdated data in the training corpus, and is assumed to reflect the model’s intrinsic limitations [27, 14, 13, 25]. Nonetheless, such internal confusion, and consequently hallucinations, can also stem from **external uncertainty**, which occurs when the user’s query is ambiguous, such as lacking context or having multiple possible interpretations due to typos, missing information, or ambiguous

*Work done during internship at Amazon. Correspondence to: Xiaomin Li (email: xiaominli@g.harvard.edu)

entities [47, 36, 26, 24, 12, 29]. Cases of external uncertainty should be handled separately by requesting clarification from the user [47, 36, 26, 29]. For example, when asked the ambiguous question “Who played Spiderman?”, an LLM should ask the user to specify which movie they are referring to. It is important to note that internal uncertainty reflects true limitations of the model only after external uncertainty has been ruled out. To detect external uncertainty (query ambiguity), current methods often rely on LLMs themselves to assess ambiguity via specialized prompting strategies [26, 24, 12, 47]. In contrast, internal uncertainty (response uncertainty) detection follows two main paradigms: 1. **Probability-based** methods that utilize the token probabilities or entropy, requiring internal access to the model [23, 35, 38, 22]. 2. **Sampling-based** approaches, which sample multiple responses and propose measures to quantify uncertainty [13, 15, 46, 27, 14, 25, 32]. A representative method in this category is the *Semantic Entropy*, which clusters sampled responses into semantic equivalence classes and computes entropy across these clusters [27, 14].

In this work, we introduce a unified sampling-based approach called the *Semantic Volume*, which can generally be applied to detect both internal and external uncertainty in LLMs (see Figure 1). Our method generates perturbations of queries and responses, obtains their semantic embedding vectors, and use a mathematical measure that essentially computes the determinant of the Gram matrix formed by the vectors, in order to quantify the semantic dispersion. Larger dispersion indicates higher uncertainty. More precisely, for external uncertainty, we prompt the LLM to generate multiple augmented versions of each query as perturbations, while for internal uncertainty, we sample multiple responses as perturbations. Then we take the normalized embedding vectors to be their representations. Putting these vectors as column vectors in a matrix V , the value $\det(V^\top V)$ mathematically measures the squared volume of the parallelepiped formed by these vectors. The log of this value essentially defines our Semantic Volume (see 3.1). The idea is that if uncertainty is low, all perturbations should be similar or close to each other, resulting in a small dispersion (i.e., a smaller volume).

We conduct comprehensive experiments on both query ambiguity detection and response uncertainty detection, demonstrating that our semantic volume method outperforms various baselines in both tasks. Additionally, we provide theoretical justification showing that our measure essentially captures the differential entropy of perturbation vectors, effectively quantifying overall semantic dispersion. Notably, semantic entropy emerges as a special case of our approach, highlighting the broader generalization of semantic volume over existing sampling-based methods. Our findings suggest that semantic volume provides a robust, interpretable framework for improving LLM reliability by systematically detecting and addressing uncertainty in both user queries and model responses. Below is a list of our main contributions:

- We propose a novel mathematical measure for uncertainty detection, using the determinant of the Gram matrix (equivalently, parallelepiped volume) of embedding vectors to quantify semantic dispersion.
- Our method is **training-free** and **does not require internal access** to the model’s internal states or token probabilities).
- To the best of our knowledge, this is the **first framework to study both external and internal uncertainty** in LLMs.
- We validate our approach through comprehensive experiments on both external and internal uncertainty detection, demonstrating superior performance compared to various baselines ².
- We provide **theoretical interpretations** of our semantic volume, linking it to differential entropy and generalizing existing sampling-based uncertainty measures.

2 Related Work

2.1 Hallucination

LLM hallucinations occur when the model generates incorrect, incomplete, fabricated, or misleading outputs [21, 20, 8, 17, 11]. Generally the hallucination can be caused by the lack of knowledge of the LLM itself (internal uncertainty), but could also originate from the ambiguity in the user’s query (external uncertainty). Most LLMs are not explicitly trained to handle ambiguous queries

²Code of our experiments: <https://anonymous.4open.science/r/LLMUncertainty-5C61>.

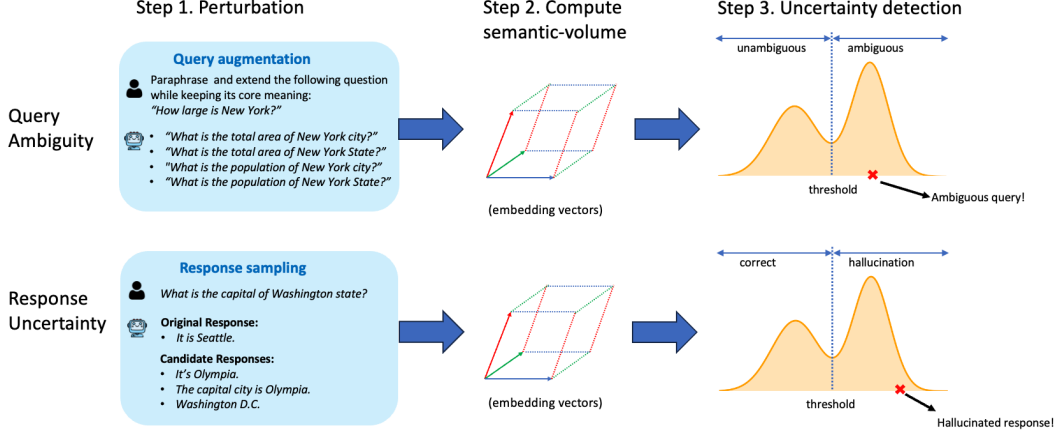


Figure 1: Pipeline for external and internal uncertainty detection using semantic volume. *Step 1.* Generate perturbations. For external uncertainty, we augment each query using an LLM, treating the augmentations as perturbations. For internal uncertainty, perturbations refer to multiple sampled candidate responses. *Step 2.* Compute semantic volume (essentially $\log \det(\mathbf{V}^\top \mathbf{V})$ where columns of \mathbf{V} are normalized embedding vectors). *Step 3.* Cases with high semantic volume are predicted as ambiguous queries (external uncertainty) or hallucinated responses (internal uncertainty).

and often generate incorrect responses instead, leading to hallucinations [24]. Addressing external uncertainty requires a different approach, such as prompting the LLM to ask clarification questions before generating a response [47, 36, 26, 29]. In contrast, internal uncertainty caused by knowledge gaps can be mitigated through methods like retrieval-augmented generation for additional context [30], reasoning-based techniques to improve understanding [43, 18, 37], or simply turning to stronger LLMs or human agents.

2.2 External Uncertainty

Query ambiguity detection is typically performed using LLMs with various prompting techniques [26, 24, 36, 47, 12, 45, 29]. For instance, Kuhn et al. [26] use LLM prompting for both detecting ambiguity and generating clarification questions. Kim et al. [24] prompts LLM to disambiguate question x itself, and then measure the difference between the x_{new} and x . Larger difference above a threshold indicates ambiguity. Min et al. [36] introduced the AmbigNQ dataset, which contains ambiguous queries and their answers. Building on this, Zhang et al. [47] proposed a taxonomy for different types of query ambiguity and released the CLAMBER benchmark, which provides binary labels indicating whether a query is ambiguous. They further evaluated various models on ambiguity detection under different settings, including zero-shot vs. few-shot and chain-of-thought (CoT) prompting vs. standard prompting.

2.3 Internal Uncertainty

There is a growing stream of works proposing uncertainty measures to detect hallucination [27, 14, 13, 23, 35, 15, 25, 32, 33, 38] (similar to all these studies, we focus on scenarios where the LLM exhibits high uncertainty when making mistakes, and cases where an LLM hallucinates with high confidence are beyond the scope of this paper). There are generally two genres: **Probability-based**, using information such as the token probability or entropy, and **Sampling-based**, which samples more responses and measure the dispersion of the answers.

Probability-based. *Last Token Entropy*, which essentially uses the entropy of the vocabulary distribution at the last token, is a widely used measure of uncertainty [35]. *Log Probabilities* average the log of the conditional probabilities of the tokens (equivalently the log of the products of consecutive token probabilities) [35, 38]. Quevedo et al. [38] tries multiple ways to aggregate the token probabilities, such as the minimal and averaged token probabilities.

Sampled-based. Kuhn et al. [27] proposed *Semantic Entropy* to measure uncertainty in natural language and Farquhar et al. [14] applied it to detect hallucinations in large language models. Essentially for each query, they generate multiple answers, and then cluster them by the same semantic meanings. Then discrete entropy calculated from the sizes of different clusters is defined as the semantic entropy. In Kadavath et al. [23] and Cole et al. [13], they sample multiple answers and let LLM to judge the uncertainty based on these answers. This method is called $p(\text{True})$ in Kuhn et al. [27]. The *Lexical Similarity* method [15, 16] considers the averaged similarity of the sampled answers, and lower similarity indicates higher dispersion.

3 Method

3.1 Definitions and Notations:

Denote $[k] \stackrel{\text{def}}{=} \{1, 2, \dots, k\}$ for any $k \in \mathbb{N}$. For the task of external uncertainty detection, we denote the query dataset by $\mathcal{D}_Q = \{q_i\}_{i \in [N_Q]}$, along with a tiny labeled subset $\mathcal{L}_Q \subseteq \mathcal{D}_Q$ (used to determine optimal semantic volume threshold and each query is assigned a binary label indicating whether it is ambiguous). For internal uncertainty detection, we define the query-response dataset as $\mathcal{D}_R = \{(q_i, r_i)\}_{i \in [N_R]}$ with a labeled subset $\mathcal{L}_R \subseteq \mathcal{D}_R$. Since our method and analysis apply to both tasks, we often drop the subscript and use the general notation $\mathcal{D} = \{s_i\}_{i \in [N]}$ and $\mathcal{L} \in \mathcal{D}$, where s_i represents a query for external uncertainty and a query-response pair for internal uncertainty.

Volume. Given normalized embedding vectors $\mathbf{V} = [\mathbf{v}_1 \mathbf{v}_2 \dots \mathbf{v}_n]$ (each $\|\mathbf{v}_i\| = 1$), we define the squared volume as:

$$\text{Vol}^2(\mathbf{V}) \stackrel{\text{def}}{=} \det(\mathbf{V}^\top \mathbf{V}). \quad (1)$$

The term ‘‘volume’’ originates from the fact that geometrically, $\sqrt{\det(\mathbf{V}^\top \mathbf{V})}$ represents the volume of the parallelepiped spanned by vectors $\{\mathbf{v}_i\}$. For example, in the three-dimensional case, where $\mathbf{V} = [\mathbf{v}_1 \mathbf{v}_2 \mathbf{v}_3]$, it can be verified that $\sqrt{\det(\mathbf{V}^\top \mathbf{V})}$ precisely computes $|\mathbf{v}_1^\top (\mathbf{v}_2 \times \mathbf{v}_3)|$, which corresponds to the volume of the three-dimensional parallelepiped formed by $\{\mathbf{v}_1, \mathbf{v}_2, \mathbf{v}_3\}$. A more detailed discussion on the geometric interpretation of this measure is provided in Appendix B).

Semantic Volume. A key limitation of equation 1 is that if duplicate embeddings exist in \mathbf{V} (e.g., two sampled responses or extended queries are identical), then $\det(\mathbf{V}^\top \mathbf{V})$ is immediately zero because $\mathbf{V}^\top \mathbf{V}$ is singular. To address this, we introduce a small perturbation $\epsilon \mathbf{I}$ with $\epsilon = 10^{-10}$ and compute $\det(\mathbf{V}^\top \mathbf{V} + \epsilon \mathbf{I})$ to maintain numerical stability (in Appendix D, we show that ϵ is negligible to the spectral norm $\|\mathbf{V}^\top \mathbf{V}\|$ and hence it only serves to ensure numerical stability and does not affect the quantification). In practice, the absolute values of squared volumes are often small due to the nature of our perturbations. Therefore we take the logarithm, leading to the formulation

$$\log \text{Vol}^2(\mathbf{V}) \stackrel{\text{def}}{=} \log \det(\mathbf{V}^\top \mathbf{V} + \epsilon \mathbf{I}_n) \quad (2)$$

Moreover, we apply Principal Component Analysis (PCA) to reduce dimensionality by projecting the vectors onto the top d principal components, obtaining $\tilde{\mathbf{V}} = [\tilde{\mathbf{v}}_1 \tilde{\mathbf{v}}_2 \dots \tilde{\mathbf{v}}_n] \in \mathbb{R}^{d \times n}$, where each $\tilde{\mathbf{v}}_i \stackrel{\text{def}}{=} \mathbf{P}_{PCA} \mathbf{v}_i$. Here, \mathbf{P}_{PCA} is the projection matrix. This results in the general form of our final semantic volume measure:

$$\text{SemanticVolume}(\mathbf{V}) \stackrel{\text{def}}{=} \log \text{Vol}^2(\mathbf{P}_{PCA} \mathbf{V}) = \log \det(\tilde{\mathbf{V}}^\top \tilde{\mathbf{V}} + \epsilon \mathbf{I}_n) \quad (3)$$

3.2 Semantic Volume Uncertainty Detection Algorithm:

Our algorithm using semantic volume to detect high uncertainty is outlined below (the overall pipeline is illustrated in Figure 1 and the detailed pseudocode is provided in Algorithm 1).

Step 1: Augmentation. For each $s \in \mathcal{D}$, we augment it with n perturbations. Precisely, for external uncertainty, we prompt an LLM to augment/paraphrase each query s to obtain n perturbed versions, while for internal uncertainty, we sample n candidate responses.

Step 2: Compute semantic volume. We obtain embedding vectors using Sentence-Transformer [39], normalize them, and apply PCA dimension reduction, yielding $\tilde{\mathbf{V}} = [\tilde{\mathbf{v}}_1 \tilde{\mathbf{v}}_2 \dots \tilde{\mathbf{v}}_n] \in \mathbb{R}^{d \times n}$ for n perturbations. Then compute the semantic volume according to equation 3.

Step 3: Uncertainty detection. A higher semantic volume indicates greater uncertainty. To determine the optimal threshold τ^* , we use a tiny labeled random subset $\mathcal{L} \subseteq \mathcal{D}$ with size 100 for threshold tuning³ (the exact formula for τ^* is characterized in Proposition 1). Finally, we classify the entire dataset \mathcal{D} by assigning binary uncertainty labels based on the semantic volume threshold.

4 Experiment: External Uncertainty

4.1 Experimental Setup

Data. We use the CLAMBER dataset[47], a benchmark for evaluating LLM queries using a well-organized taxonomy. It is a balanced dataset containing 3K queries, each annotated with a binary label indicating whether it is ambiguous.

Models. For query augmentation, we use Claude3.5-Sonnet [6] and the prompt is provided in Appendix J. Qwen2-1.5B-instruct [44] is used as the sentence-transformer to generate embeddings.

Evaluation. We conduct experiments for binary classification task on ambiguity of the queries. The performance is assessed by comparing the predicted binary labels against the ground truth labels, reporting both accuracy and F1 score.

Baselines. Note that the sampling-based methods discussed in Section 2.3 can be naturally extended to query ambiguity detection if we can generate analogous perturbations of the queries, similar to how candidate responses are sampled in response uncertainty detection. Below, we outline the baseline methods we consider. Some of these were originally designed for response uncertainty, but we readily adapt their methodology to query ambiguity.

- *Type 1: Prompting-based.* Directly prompt LLMs to determine whether a given query is ambiguous. We evaluate the following models: Vicuna-13B [34], Llama2-13B [42], Llama2-70B [42], Llama3.2-3B [2], and ChatGPT [1]. Additionally, we include results for ChatGPT with few-shot learning and chain-of-thought reasoning, as reported in the original CLAMBER paper [47].
- *Type 2: Probability-based.* Using the token probabilities to quantify uncertainty. Note that these methods typically require direct access to the model’s internal probability distributions. We consider the follow methods and use Llama3.2-1B-Instruct [2] to obtain the token probabilities. (a) **Last Token Entropy** [23, 7, 35]: computes the entropy of the vocabulary distributions at the last token of the query. (b) **Log Probabilities** [35, 38]: measures uncertainty by computing the log of the product of conditional token probabilities, which is equivalent to summing the log conditional probabilities across all tokens in the query.
- *Type 3: Sampling-based.* These methods employ a perturbation approach similar to ours. The original text is perturbed to generate multiple variations, and the uncertainty is quantified by measuring the variation among the generated samples. (a) **p(True)** [23, 13]: the original p(True) method quantifies uncertainty based on the probability of the LLM’s output. Instead, we directly use the LLM’s answer and compare it against the ground truth binary labels. (b) **Lexical Similarity** [32, 15]: computes the averaged pairwise similarity of perturbed queries. (c) **Semantic Entropy** [27]: clusters the perturbations into semantic equivalence classes and computes the entropy over the clusters.

4.2 Results

The performance of our method and baseline approaches on the query ambiguity classification task is presented in Table 1. Here we choose $n = 20$ for the augmentations for queries (the discussion on varying the perturbation size n is provided in Appendix F). The original CLAMBER dataset includes a diverse range of ambiguities, such as queries involving unfamiliar entities, self-contradictions, multiple meanings, and missing context (e.g., personal, temporal, spatial, or task-specific). We observe that identifying ambiguous queries remains challenging for LLMs, even for powerful models like ChatGPT, despite various prompting strategies (few-shot and CoT). Among the baselines, probability-based methods achieve higher F1 scores but a critical limitation of them is that they

³Note that this labeled subset is only used for finding a more precise threshold. In practice, one can consider a completely unsupervised setting and use a simpler heuristic threshold such as the median.

require access to token probabilities, which is not provided for most of the close-sourced models. Among sampling-based methods, semantic entropy generally performs better. Nonetheless, our semantic volume method significantly outperforms all three categories of baselines, demonstrating its effectiveness in detecting ambiguous queries.

Method	Accuracy	F1
Vicuna-13B (zero-shot)	50.6	39.9
Llama2-13B (zero-shot)	45.6	43.6
Llama2-70B (zero-shot)	50.3	34.2
Llama3.2-3B (zero-shot)	51.5	37.7
ChatGPT (zero-shot)	54.3	53.4
ChatGPT (few-shot)	51.6	49.2
ChatGPT (zero-shot + CoT)	<u>57.3</u>	56.9
ChatGPT (few-shot + CoT)	53.6	51.4
Last Token Entropy	52.2	<u>67.3</u>
Log Probabilities	45.5	66.0
pTrue (Llama3-8B)	52.5	53.3
pTrue (Mistral-7B)	47.1	26.6
Lexical Similarity	52.7	53.6
Semantic Entropy	50.1	62.8
Semantic Volume (ours)	58.0	69.0

Table 1: External Uncertainty: Performance comparison based on Accuracy and F1 score.

5 Experiment: Internal Uncertainty

5.1 Experimental Setup

Data. We use a subset of the TriviaQA dataset[47], a reading comprehension dataset containing questions with reference answers. We generate responses using Llama3.2-1B-Instruct at zero temperature and a response y is flagged as a hallucination if the ROUGE-L score with respect to the reference answer y_{ref} falls below 0.3 (i.e. the label is defined as $\mathbf{1}_{RougeL(y, y_{ref}) < 0.3}$), following the same metric used in Kosken et al. [25]. This process yields the hallucination labels for the dataset. We retain 2500 data labeled as hallucinations and 2500 labeled as correct, constructing a balanced 5K dataset with binary hallucination labels.

Models. For sampling-based methods, we generate candidate responses from the same Llama3.2-1B-Instruct with temperature 1. For embeddings, we use the same sentence-transformer as in Section 4.

Evaluation. We compare the predicted binary hallucination labels against the ground truth labels and report both accuracy and F1 score. Furthermore, we also add the evaluation based on the AUROC (area under the receiver operator characteristic curve) metric, which compares the raw uncertainty scores against the ground truth labels. In fact, for a given uncertainty measure $m(\cdot)$, the AUROC score is equivalent to $\mathbb{P}[m(y_{hallucinated}) > m(y_{correct})]$, where $y_{hallucinated}$ and $y_{correct}$ are randomly chosen hallucinated and correct answers, respectively. Hence a higher AUROC (closer to 1) indicates that the uncertainty measure more effectively distinguishes hallucinated responses by assigning them higher uncertainty scores. AUROC is a widely used metric in many existing studies on response hallucination detection [27, 25, 23].

Baselines. We adapt the baseline methods from Section 4.1, applying them to sampled responses instead of augmented queries.

5.2 Results

The performance results are presented in Tables 2 and 3. For sampling-based methods, we set the response sampling size to $n = 20$. Notably, our semantic volume method significantly outperforms all baselines in both accuracy and F1 score. Furthermore, the AUROC results in Table 3 confirm that our semantic volume serves as a highly effective uncertainty signal for hallucination detection. Additionally, we observe that when comparing p(True), which includes sampled candidate responses

as context, to direct prompting, the inclusion of context degrades the performance. Moreover, for methods that rely on prompting LLMs (including pTrue), we find that LLMs sometimes exhibit a strong bias toward answering almost all “Yes” or all “No”. In fact in Table 2, both *Prompt Llama3.2-1B* and *pTrue (Llama3.2-1B)* exhibit this behavior, nearly predicting all response as hallucinations (further discussions are provided in Appendix H). This instability highlights another drawback of such methods that rely on LLM prompting for uncertainty estimation. From both tables, we observe that sampling-based methods that measure the dispersion of sampled responses (particularly lexical similarity and semantic entropy) generally outperform probability-based methods, which aligns with the findings in Cole et al. [13].

Method	Accuracy	F1
Prompt Llama3.2-1B	50.5	66.8
Prompt Llama3-8B	65.5	60.1
Prompt Mistral-7B	68.7	61.8
Last Token Entropy	60.1	59.9
Log Probabilities	60.1	62.9
pTrue (Llama3.2-1B)	49.6	64.0
pTrue (Llama3-8B)	63.7	45.4
pTrue (Mistral-7B)	62.9	45.8
Lexical Similarity	64.2	72.0
Semantic Entropy	63.5	69.4
Semantic Volume (ours)	72.8	75.4

Table 2: Internal Uncertainty: Performance comparison based on Accuracy and F1 score.

Method	AUROC
Last Token Entropy	63.9
Log Probabilities	65.5
pTrue (Llama3.2-1B)	61.3
pTrue (Llama3-8B)	58.3
pTrue (Mistral-7B)	65.4
Lexical Similarity	73.4
SemanticEntropy	73.4
Semantic Volume (ours)	79.6

Table 3: Internal Uncertainty: Performance comparison based on AUROC.

5.3 Distribution Separation

In this section, we compare the distributions of various uncertainty measures using both visualization and the Kolmogorov–Smirnov (KS) test [4, 40]. Specifically, we plot histograms for the hallucinated subset (hallucination label = 1) and the correct subset (hallucination label = 0) from our TriviaQA dataset. Ideally, a well-performing measure should yield two distinct bulks, with greater separation indicating stronger discriminative power. To quantitatively assess the separation, we perform a two-sample Kolmogorov–Smirnov test, a non-parametric test that compares two empirical distributions by measuring the maximum distance between their empirical cumulative distribution functions (ECDFs). A large KS statistic combined with a small p -value suggests that the two distributions are significantly different.

The plots and statistics are shown in Figure 2. Combined the KS statistics and the histograms, we observe that indeed *Last Token Entropy* and *Log Probabilities* struggle to effectively separate the two groups of data, while *Lexical Similarity*, *Semantic Entropy*, and our *Semantic Volume* exhibit stronger separation. Particularly, we note that the distribution of semantic entropy closely resembles that of our semantic volume measure. In fact, we will provide theoretical analysis in Section 7 showing that our semantic volume can be interpreted as the differential entropy of the semantic embedding vectors, and can be viewed as a more general and continuous version of semantic entropy.

6 Ablation Study and Hyperparameter Analysis

The original embedding dimension from the sentence-transformer is 1536. In the external uncertainty experiment, we reduce the dimensionality using PCA with $d = 10$, while in the internal uncertainty experiment, we set $d = 20$. To assess the impact of this reduction, we conduct an ablation study, demonstrating that using the projected vectors \tilde{V} leads to better performance than the original raw embeddings V (see Appendix E). This suggests that lower-dimensional projections help separate perturbation vectors more effectively. Furthermore, we explore various values of d to analyze the effect of dimensionality on performance. Our findings indicate that the optimal dimension d is task-dependent, with diminishing improvements beyond a certain point. Nonetheless, it is important to note that even without PCA dimension reduction, our method still outperforms various baselines in both external and internal uncertainty detection tasks.

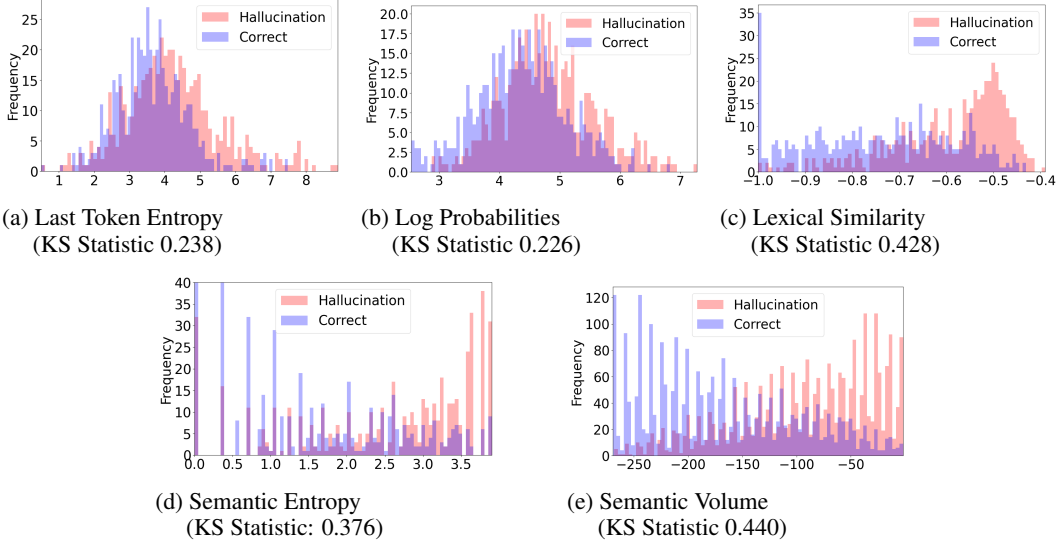


Figure 2: Distribution of subsets for both labels across different uncertainty measures. Two-sample Kolmogorov–Smirnov statistics are computed to quantify the separation of two bulks (all p -values of them are less than 10^{-11}).

To demonstrate the generalizability of our method and study the effect of various hyperparameters and model choices. In Appendix F, we analyze the effect of varying n , the number of perturbations. As expected, larger n yields more accurate uncertainty estimation but increases computational cost, while smaller n reduces cost but may sacrifice accuracy. We choose $n = 20$ to balance performance and efficiency. In Appendices G and H, we examine the impact of different embedding models and response generation models. We find that larger embedding models provide little additional performance gain. Furthermore, when detecting hallucinations in responses generated by a larger LLM, the performance of most methods slightly declines. However, our Semantic Volume method still outperforms all baselines.

7 Theoretical Analysis

In this section, we present theoretical analyses, with proofs and additional supporting lemmas provided in Appendix C. First, we derive the exact formula for the optimal threshold τ^* in Proposition 1. Then in Theorem 1 and Theorem 2, we show that under the assumption that the perturbations follow a Gaussian distribution, our semantic volume measure effectively computes the differential entropy of the embedding vectors, using entropy as a measure of uncertainty detection. This insight allows us to naturally view our method as a generalization of semantic entropy [27]. Notably, semantic entropy involves a manual clustering step, and only considers the entropy between clusters while ignoring discrepancies within clusters (since the responses in the same cluster are semantically similar but not exactly identical). In contrast, **our method more generally captures the overall semantic dispersion across all sampled perturbations**, providing a more comprehensive uncertainty measure.

Proposition 1 (Formula for optimal threshold τ^*). *Denote $\mathcal{L} \in \mathcal{D}$ as a labeled subset with inputs $\{s_i\}$ and labels $\{y_i\}$:*

$$\mathcal{L} = \{(s_i, y_i)\}_{i=1}^M \quad \text{with} \quad y_i \in \{0, 1\},$$

For each s_i , denotes its semantic volume as $m(s_i)$. Define a classification rule

$$\hat{y}_i(\tau) = \begin{cases} 1, & m(s_i) > \tau, \\ 0, & \text{otherwise.} \end{cases}$$

Then the optimal threshold τ that maximizes the F_1 score on \mathcal{L} is given by

$$\tau^* \stackrel{\text{def}}{=} \arg \max_{\tau \in \mathbb{R}} F_1(\tau) = \arg \max_{\tau \in \mathbb{R}} \left(\frac{2 \sum_{i=1}^M \mathbf{1}_{\hat{y}_i(\tau)=y_i=1}}{\sum_{i=1}^M \mathbf{1}_{\hat{y}_i(\tau)=1} + \mathbf{1}_{y_i=1}} \right). \quad (4)$$

Note that the F_1 score can be replaced by other metrics, such as the accuracy.

Theorem 1. Denote the embedding vector and normalized embedding vector of the original text (either a query or a response) as $\bar{\mathbf{x}}$ and $\bar{\mathbf{v}}$, respectively. Denote the perturbation embeddings as $\mathbf{X} \stackrel{\text{def}}{=} [\mathbf{x}_1 \mathbf{x}_2 \dots \mathbf{x}_n] \in \mathbb{R}^{d \times n}$ and the normalized perturbation embeddings as $\mathbf{V} \stackrel{\text{def}}{=} [\mathbf{v}_1 \mathbf{v}_2 \dots \mathbf{v}_n] \in \mathbb{R}^{d \times n}$ (i.e. $\mathbf{x}_i = \mathbf{v}_i / \|\mathbf{v}_i\|$ for each $i \in [n]$). Assume Gaussian distribution $\mathbf{x}_i \sim \mathcal{N}(\bar{\mathbf{x}}, \Sigma)$. Then in high-dimensional regime, $\log \det(\mathbf{V}^\top \mathbf{V})$ corresponds to the shifted differential entropy of the perturbations $\{\mathbf{x}_i\}_{i \in [n]}$. That is,

$$\log \det(\mathbf{V}^\top \mathbf{V}) \doteq \mathcal{H}(\mathbf{X}) + C,$$

where $\mathcal{H}(\mathbf{X}) \stackrel{\text{def}}{=} -\mathbb{E}_{x \sim \mathbf{X}} [\log p_{\mathbf{X}}(x)]$ is the differential entropy and C is a constant offset term.

Then we obtain the following Theorem, which is a direct consequence of Theorem 1 and Lemma 1 in Appendix C.

Theorem 2. Under the same setting and notations of the Theorem 1, our **Semantic Volume** method essentially generates same binary decisions compared to using **differential entropy** of the perturbation embedding vectors. That is, denote the Semantic Volume measure and differential entropy measure as $m(\cdot)$ and $\tilde{m}(\cdot)$ respectively. For the labels

$$y_i \stackrel{\text{def}}{=} \mathbf{1}_{m(s_i) < \tau^*} \quad \text{and} \quad \tilde{y}_i \stackrel{\text{def}}{=} \mathbf{1}_{\tilde{m}(s_i) < \tilde{\tau}^*},$$

where $\tilde{\tau}^*$ is the optimal threshold for the differential entropy measure, we have

$$\tilde{y}_i = y_i \quad \text{for all } s_i \in \mathcal{D} \setminus \mathcal{L}.$$

8 Conclusion

One limitation of our current study is that our work considers the same scope as the references in 2.3: we focus on the situation where uncertainty aligns with incorrectness, without addressing *confidently wrong* responses, meaning an LLM hallucinates with high confidence (low uncertainty). We believe that addressing such cases requires different strategies, such as factuality checking, detecting self-contradictions in chain-of-thought reasoning or incorporating external knowledge for verification. We leave these explorations for future work.

In summary, we have introduced *Semantic Volume*, a novel and general-purpose measure for detecting both *external uncertainty* (query ambiguity) and *internal uncertainty* (response uncertainty) in large language models. By generating perturbations, embedding these perturbations as normalized vectors, and computing the determinant of their Gram matrix, we obtain a measure that captures the overall semantic dispersion. Extensive experiments on benchmark datasets showed that semantic volume significantly outperforms various types of existing baselines (prompting-based, probability-based, and sampling-based) for both ambiguous query classification and response hallucination detection. Furthermore, from a theoretical standpoint, we established that semantic volume can be viewed as the differential entropy of the embedding vectors, thereby unifying and extending prior sampling-based metrics (e.g., semantic entropy). This interpretation highlights why our measure is robust and comprehensive: unlike purely clustering-based approaches, we account for the *overall* dispersions in the embedding space. Moreover, our method is applicable even when the LLM is only accessible via an external API or when internal model details are unavailable, making it broadly practical across closed-source or API-based models. Overall, our findings suggest that semantic volume is a promising step toward more reliable, interpretable uncertainty detection for both external and internal uncertainty of LLMs.

References

- [1] Josh Achiam, Steven Adler, Sandhini Agarwal, Lama Ahmad, Ilge Akkaya, Florencia Leoni Aleman, Diogo Almeida, Janko Altenschmidt, Sam Altman, Shyamal Anadkat, et al. Gpt-4 technical report. *arXiv preprint arXiv:2303.08774*, 2023.
- [2] Meta AI. Llama 3.2: Advancing ai for vision, edge, and mobile devices. Meta AI Blog, 2024. URL <https://ai.meta.com/blog/llama-3-2-connect-2024-vision-edge-mobile-devices/>. Accessed: Feb 11, 2025.

- [3] AI@Meta. Llama 3 model card. 2024. URL https://github.com/meta-llama/llama3/blob/main/MODEL_CARD.md.
- [4] Kolmogorov An. Sulla determinazione empirica di una legge didistribuzione. *Giorn Dell'inst Ital Degli Att*, 4:89–91, 1933.
- [5] Rohan Anil, Sebastian Borgeaud, Yonghui Wu, Jean-Baptiste Alayrac, Jiahui Yu, Radu Soricut, Johan Schalkwyk, Andrew M Dai, Anja Hauth, Katie Millican, et al. Gemini: A family of highly capable multimodal models. *arXiv preprint arXiv:2312.11805*, 2023.
- [6] Anthropic. Introducing the Claude 3 family of models, 2023. URL <https://www.anthropic.com/news/clause-3-family>. Accessed: 2025-01-02.
- [7] Udit Arora, William Huang, and He He. Types of out-of-distribution texts and how to detect them. *arXiv preprint arXiv:2109.06827*, 2021.
- [8] Yejin Bang, Samuel Cahyawijaya, Nayeon Lee, Wenliang Dai, Dan Su, Bryan Wilie, Holy Love-nia, Ziwei Ji, Tiezheng Yu, Willy Chung, et al. A multitask, multilingual, multimodal evaluation of chatgpt on reasoning, hallucination, and interactivity. *arXiv preprint arXiv:2302.04023*, 2023.
- [9] Alexander Bastounis, Paolo Campodonico, Mihaela van der Schaar, Ben Adcock, and Anders C Hansen. On the consistent reasoning paradox of intelligence and optimal trust in ai: The power of ‘i don’t know’. *arXiv preprint arXiv:2408.02357*, 2024.
- [10] Tom B Brown. Language models are few-shot learners. *arXiv preprint arXiv:2005.14165*, 2020.
- [11] Xiuying Chen, Mingzhe Li, Xin Gao, and Xiangliang Zhang. Towards improving faithfulness in abstractive summarization. *Advances in Neural Information Processing Systems*, 35:24516–24528, 2022.
- [12] Yizhou Chi, Jessy Lin, Kevin Lin, and Dan Klein. Clarinet: Augmenting language models to ask clarification questions for retrieval. *arXiv preprint arXiv:2405.15784*, 2024.
- [13] Jeremy R Cole, Michael JQ Zhang, Daniel Gillick, Julian Martin Eisenschlos, Bhuwan Dhingra, and Jacob Eisenstein. Selectively answering ambiguous questions. *arXiv preprint arXiv:2305.14613*, 2023.
- [14] Sebastian Farquhar, Jannik Kossen, Lorenz Kuhn, and Yarin Gal. Detecting hallucinations in large language models using semantic entropy. *Nature*, 630(8017):625–630, 2024.
- [15] Marina Fomicheva, Shuo Sun, Lisa Yankovskaya, Frédéric Blain, Francisco Guzmán, Mark Fishel, Nikolaos Aletras, Vishrav Chaudhary, and Lucia Specia. Unsupervised quality estimation for neural machine translation. *Transactions of the Association for Computational Linguistics*, 8:539–555, 2020.
- [16] Yashvir S Grewal, Edwin V Bonilla, and Thang D Bui. Improving uncertainty quantification in large language models via semantic embeddings. *arXiv preprint arXiv:2410.22685*, 2024.
- [17] Nuno M Guerreiro, Duarte M Alves, Jonas Waldendorf, Barry Haddow, Alexandra Birch, Pierre Colombo, and André FT Martins. Hallucinations in large multilingual translation models. *Transactions of the Association for Computational Linguistics*, 11:1500–1517, 2023.
- [18] Daya Guo, Dejian Yang, Haowei Zhang, Junxiao Song, Ruoyu Zhang, Runxin Xu, Qihao Zhu, Shirong Ma, Peiyi Wang, Xiao Bi, et al. Deepseek-r1: Incentivizing reasoning capability in llms via reinforcement learning. *arXiv preprint arXiv:2501.12948*, 2025.
- [19] David A Harville. Matrix algebra from a statistician’s perspective, 1998.
- [20] Lei Huang, Weijiang Yu, Weitao Ma, Weihong Zhong, Zhangyin Feng, Haotian Wang, Qian-glong Chen, Weihua Peng, Xiaocheng Feng, Bing Qin, et al. A survey on hallucination in large language models: Principles, taxonomy, challenges, and open questions. *arXiv preprint arXiv:2311.05232*, 2023.

[21] Ziwei Ji, Nayeon Lee, Rita Frieske, Tiezheng Yu, Dan Su, Yan Xu, Etsuko Ishii, Ye Jin Bang, Andrea Madotto, and Pascale Fung. Survey of hallucination in natural language generation. *ACM Computing Surveys*, 55(12):1–38, 2023.

[22] Ziwei Ji, Delong Chen, Etsuko Ishii, Samuel Cahyawijaya, Yejin Bang, Bryan Wilie, and Pascale Fung. Llm internal states reveal hallucination risk faced with a query. *arXiv preprint arXiv:2407.03282*, 2024.

[23] Saurav Kadavath, Tom Conerly, Amanda Askell, Tom Henighan, Dawn Drain, Ethan Perez, Nicholas Schiefer, Zac Hatfield-Dodds, Nova DasSarma, Eli Tran-Johnson, et al. Language models (mostly) know what they know. *arXiv preprint arXiv:2207.05221*, 2022.

[24] Hyuhng Joon Kim, Youna Kim, Cheonbok Park, Junyeob Kim, Choonghyun Park, Kang Min Yoo, Sang-goo Lee, and Taeuk Kim. Aligning language models to explicitly handle ambiguity. *arXiv preprint arXiv:2404.11972*, 2024.

[25] Jannik Kossen, Jiatong Han, Muhammed Razzak, Lisa Schut, Shreshth Malik, and Yarin Gal. Semantic entropy probes: Robust and cheap hallucination detection in llms. *arXiv preprint arXiv:2406.15927*, 2024.

[26] Lorenz Kuhn, Yarin Gal, and Sebastian Farquhar. Clam: Selective clarification for ambiguous questions with generative language models. *arXiv preprint arXiv:2212.07769*, 2022.

[27] Lorenz Kuhn, Yarin Gal, and Sebastian Farquhar. Semantic uncertainty: Linguistic invariances for uncertainty estimation in natural language generation. *arXiv preprint arXiv:2302.09664*, 2023.

[28] Alex Kulesza, Ben Taskar, et al. Determinantal point processes for machine learning. *Foundations and Trends® in Machine Learning*, 5(2–3):123–286, 2012.

[29] Dongryeol Lee, Segwang Kim, Minwoo Lee, Hwanhee Lee, Joonsuk Park, Sang-Woo Lee, and Kyomin Jung. Asking clarification questions to handle ambiguity in open-domain qa. *arXiv preprint arXiv:2305.13808*, 2023.

[30] Patrick Lewis, Ethan Perez, Aleksandra Piktus, Fabio Petroni, Vladimir Karpukhin, Naman Goyal, Heinrich Küttler, Mike Lewis, Wen-tau Yih, Tim Rocktäschel, et al. Retrieval-augmented generation for knowledge-intensive nlp tasks. *Advances in Neural Information Processing Systems*, 33:9459–9474, 2020.

[31] Xiaomin Li, Mingye Gao, Zhiwei Zhang, Chang Yue, and Hong Hu. Rule-based data selection for large language models. *arXiv preprint arXiv:2410.04715*, 2024.

[32] Zhen Lin, Shubhendu Trivedi, and Jimeng Sun. Generating with confidence: Uncertainty quantification for black-box large language models. *arXiv preprint arXiv:2305.19187*, 2023.

[33] Linyu Liu, Yu Pan, Xiaocheng Li, and Guanting Chen. Uncertainty estimation and quantification for llms: A simple supervised approach. *arXiv preprint arXiv:2404.15993*, 2024.

[34] LMSys. Vicuna: An open-source chatbot impressing gpt-4 with 90% chatgpt quality. LMSys Blog, 2023. URL <https://lmsys.org/blog/2023-03-30-vicuna/>. Accessed: Feb 11, 2025.

[35] Andrey Malinin and Mark Gales. Uncertainty estimation in autoregressive structured prediction. *arXiv preprint arXiv:2002.07650*, 2020.

[36] Sewon Min, Julian Michael, Hannaneh Hajishirzi, and Luke Zettlemoyer. Ambigqa: Answering ambiguous open-domain questions. *arXiv preprint arXiv:2004.10645*, 2020.

[37] OpenAI. Learning to reason with llms. September 2024. <https://openai.com/index/learning-to-reason-with-llms/>.

[38] Ernesto Quevedo, Jorge Yero, Rachel Koerner, Pablo Rivas, and Tomas Cerny. Detecting hallucinations in large language model generation: A token probability approach. *arXiv preprint arXiv:2405.19648*, 2024.

[39] N Reimers. Sentence-bert: Sentence embeddings using siamese bert-networks. *arXiv preprint arXiv:1908.10084*, 2019.

[40] Nickolay Smirnov. Table for estimating the goodness of fit of empirical distributions. *The annals of mathematical statistics*, 19(2):279–281, 1948.

[41] Hugo Touvron, Thibaut Lavril, Gautier Izacard, Xavier Martinet, Marie-Anne Lachaux, Timothée Lacroix, Baptiste Rozière, Naman Goyal, Eric Hambro, Faisal Azhar, et al. Llama: Open and efficient foundation language models. *arXiv preprint arXiv:2302.13971*, 2023.

[42] Hugo Touvron, Louis Martin, Kevin Stone, Peter Albert, Amjad Almahairi, Yasmine Babaei, Nikolay Bashlykov, Siddhartha Batra, Prajjwal Bhargava, Shruti Bhosale, et al. Llama 2: Open foundation and fine-tuned chat models. *arXiv preprint arXiv:2307.09288*, 2023. URL <https://arxiv.org/abs/2307.09288>.

[43] Jason Wei, Xuezhi Wang, Dale Schuurmans, Maarten Bosma, Fei Xia, Ed Chi, Quoc V Le, Denny Zhou, et al. Chain-of-thought prompting elicits reasoning in large language models. *Advances in neural information processing systems*, 35:24824–24837, 2022.

[44] An Yang, Baosong Yang, Binyuan Hui, Bo Zheng, Bowen Yu, Chang Zhou, Chengpeng Li, Chengyuan Li, Dayiheng Liu, Fei Huang, Guanting Dong, Haoran Wei, Huan Lin, Jialong Tang, Jialin Wang, Jian Yang, Jianhong Tu, Jianwei Zhang, Jianxin Ma, Jianxin Yang, Jin Xu, Jingren Zhou, Jinze Bai, Jinzheng He, Junyang Lin, Kai Dang, Keming Lu, Keqin Chen, Kexin Yang, Mei Li, Mingfeng Xue, Na Ni, Pei Zhang, Peng Wang, Ru Peng, Rui Men, Ruize Gao, Runji Lin, Shijie Wang, Shuai Bai, Sinan Tan, Tianhang Zhu, Tianhao Li, Tianyu Liu, Wenbin Ge, Xiaodong Deng, Xiaohuan Zhou, Xingzhang Ren, Xinyu Zhang, Xipin Wei, Xuancheng Ren, Xuejing Liu, Yang Fan, Yang Yao, Yichang Zhang, Yu Wan, Yunfei Chu, Yuqiong Liu, Zeyu Cui, Zhenru Zhang, Zhifang Guo, and Zhihao Fan. Qwen2 technical report, 2024. URL <https://arxiv.org/abs/2407.10671>.

[45] Zhangyue Yin, Qiushi Sun, Qipeng Guo, Jiawen Wu, Xipeng Qiu, and Xuanjing Huang. Do large language models know what they don’t know? *arXiv preprint arXiv:2305.18153*, 2023.

[46] Michael JQ Zhang and Eunsol Choi. Clarify when necessary: Resolving ambiguity through interaction with lms. *arXiv preprint arXiv:2311.09469*, 2023.

[47] Tong Zhang, Peixin Qin, Yang Deng, Chen Huang, Wenqiang Lei, Junhong Liu, Dingnan Jin, Hongru Liang, and Tat-Seng Chua. Clamber: A benchmark of identifying and clarifying ambiguous information needs in large language models. *arXiv preprint arXiv:2405.12063*, 2024.

A Semantic-Volume Uncertainty Detection Algorithm

Here we provide the pseudocode of the Semantic-Volume uncertainty detection algorithm.

Algorithm 1 Uncertainty Detection via Semantic-Volume

Require:

- 1: • Dataset $\mathcal{D} = \{s_i\}_{i=1}^N$ of queries or query-response pairs.
- A small labeled subset $\mathcal{L} \subseteq \mathcal{D}$ with binary labels.
- SentenceTransformer model \mathcal{M} .
- 2: **for** each string $s \in \mathcal{D}$ **do**
- 3: **Extend** s via query extension/response sampling to obtain: $[s_1, s_2, \dots, s_N]$
- 4: Get normalized embedding vectors: $\mathbf{V} = [\mathbf{v}_1 \mathbf{v}_2 \dots \mathbf{v}_N] \stackrel{\text{def}}{=} \left[\frac{\mathcal{M}(s_1)}{\|\mathcal{M}s_1\|}, \frac{\mathcal{M}(s_2)}{\|\mathcal{M}s_2\|}, \dots, \frac{\mathcal{M}(s_N)}{\|\mathcal{M}s_N\|} \right]$
- 5: Apply PCA dimension reduction: $\tilde{\mathbf{V}} \stackrel{\text{def}}{=} \mathbf{P}_{PCA}\mathbf{V}$.
- 6: Compute Semantic Volume:

$$m(s) \leftarrow \log \text{Vol}(\mathbf{P}_{PCA}\mathbf{V}) \stackrel{\text{def}}{=} \log \det \left(\tilde{\mathbf{V}}^\top \tilde{\mathbf{V}} + \epsilon \mathbf{I}_n \right)$$

- 7: **end for**

- 8: **Threshold Tuning:** Using the labeled set \mathcal{L} , find the threshold τ^* that maximizes the F1 score:

$$\tau^* \leftarrow \arg \max_{\tau \in \mathbb{R}} F_1(\tau) \stackrel{\text{def}}{=} \arg \max_{\tau \in \mathbb{R}} \left(\frac{2 \sum_{i=1}^{|\mathcal{L}|} \mathbf{1}_{\hat{y}_i(\tau) = y_i=1}}{\sum_{i=1}^{|\mathcal{L}|} \mathbf{1}_{\hat{y}_i(\tau)=1} + \mathbf{1}_{y_i=1}} \right).$$

- 9: **for** each $(s, m(s))$ **do**
- 10: **Predict** s with:

$$\hat{y}_s \leftarrow \begin{cases} 1, & \text{if } m(s) > \tau^*, \\ 0, & \text{otherwise.} \end{cases}$$

- 11: **end for**

- 12: **return** The fully labeled dataset: $\{(s, \hat{y}_s) : s \in \mathcal{D}\}$.

Time Complexity

Most of the computational cost in our algorithm comes from perturbation sampling, similar to other sampling-based methods. Using the standard LLM implementation to generate multiple candidate sequences, the cost is equivalent to one LLM inference per data point. Embedding generation is highly efficient, taking approximately 5 minutes for our CLAMBER-3K dataset and 3 minutes for the TriviaQA-5K dataset on a single H100-80GB GPU. The computation of Semantic Volume, which involves matrix multiplication and determinant calculation for each set of perturbations, is computationally negligible (typically within seconds for the entire dataset), compared to the sampling step. This results in an overall complexity of $O(n)$ for our algorithm.

B Geometric interpretation as volume

We illustrate why $\det(\mathbf{V}^\top \mathbf{V})$ represents the squared volume using $n = 2$ and $n = 3$ as examples (see Figure 3). For $n = 2$, where $\mathbf{V} = [\mathbf{v}_1 \mathbf{v}_2]$, the volume of the parallelepiped (equivalently, the area of the parallelogram) is simply $\sin(\theta)$, where θ is the angle between \mathbf{v}_1 and \mathbf{v}_2 . In this case,

$$\mathbf{V} = \begin{bmatrix} \mathbf{v}_1^\top \mathbf{v}_1 & \mathbf{v}_1^\top \mathbf{v}_2 \\ \mathbf{v}_2^\top \mathbf{v}_1 & \mathbf{v}_2^\top \mathbf{v}_2 \end{bmatrix} = \begin{bmatrix} 1 & \cos \theta \\ \cos \theta & 1 \end{bmatrix}.$$

Therefore, $\sqrt{\det(\mathbf{V}^\top \mathbf{V})} = \sqrt{1 - \cos^2 \theta} = \sin \theta$. Similarly, for $\mathbf{V} = [\mathbf{v}_1 \mathbf{v}_2 \mathbf{v}_3]$, the $\sqrt{\det(\mathbf{V}^\top \mathbf{V})}$ exactly computes $|\mathbf{v}_1^\top (\mathbf{v}_2 \times \mathbf{v}_3)|$, which is the volume of the parallelepiped.

Beyond its geometric interpretation, $\det(\mathbf{V}^\top \mathbf{V})$ also quantifies the orthogonality of the vectors and is closely related to the determinantal point process (DPP) [28]. DPPs favor diverse or orthogonal subsets by assigning higher probabilities to sets with dissimilar elements, using determinants to

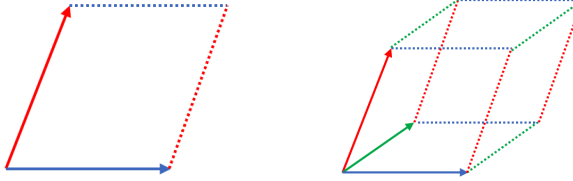


Figure 3: Parallelogram for $n = 2$ (left) and parallelepiped for $n = 3$ (right)

model repulsion among points. The Gram matrix $\mathbf{V}^\top \mathbf{V}$ is commonly used as the kernel matrix in DPPs, where the determinant of its submatrices determines subset probabilities. For a more detailed discussion, see Li et al. [31] and Kulesza et al. [28]. Moreover, some prior work has considered a similar volume measure to quantify vector diversity and orthogonality in LLM topics, such as the second orthogonality measure in [31], which motivates our design of semantic volume.

C Proofs

C.1 Proof of Proposition 1

Proof. The formula equation 4 directly follows from the definition of F_1 scores. Recall we have

$$\text{Precision}(\tau) = \frac{\text{TP}(\tau)}{\text{TP}(\tau) + \text{FP}(\tau)}, \quad \text{Recall}(\tau) = \frac{\text{TP}(\tau)}{\text{TP}(\tau) + \text{FN}(\tau)},$$

where $\text{TP}(\tau) = \sum_{i=1}^M \mathbf{1}_{\hat{y}_i(\tau)=1 \wedge y_i=1}$, $\text{FP}(\tau) = \sum_{i=1}^M \mathbf{1}_{\hat{y}_i(\tau)=1 \wedge y_i=0}$, and $\text{FN}(\tau) = \sum_{i=1}^M \mathbf{1}_{\hat{y}_i(\tau)=0 \wedge y_i=1}$. F_1 score is the harmonic mean of Precision and Recall:

$$\begin{aligned} F_1(\tau) &= 2 \cdot \frac{\text{Precision}(\tau) \times \text{Recall}(\tau)}{\text{Precision}(\tau) + \text{Recall}(\tau)} = \frac{2 \cdot \text{TP}(\tau)}{2 \cdot \text{TP}(\tau) + \text{FP}(\tau) + \text{FN}(\tau)} \\ &= \frac{2 \sum_{i=1}^M \mathbf{1}_{\hat{y}_i(\tau)=y_i=1}}{2 \sum_{i=1}^M \mathbf{1}_{\hat{y}_i(\tau)=1 \wedge y_i=1} + \sum_{i=1}^M \mathbf{1}_{\hat{y}_i(\tau)=1 \wedge y_i=0} + \sum_{i=1}^M \mathbf{1}_{\hat{y}_i(\tau)=0 \wedge y_i=1}} \\ &= \frac{2 \sum_{i=1}^M \mathbf{1}_{\hat{y}_i(\tau)=y_i=1}}{\sum_{i=1}^M (\mathbf{1}_{\hat{y}_i(\tau)=1} + \mathbf{1}_{y_i=1})}. \end{aligned}$$

□

C.2 Proof of Theorem 1

First, in Lemma 1, we formally justify that our semantic volume measure for uncertainty detection is invariant under linear transformations applied to the uncertainty measure. This invariance follows directly from the step of searching for optimal threshold τ^* in our method.

Lemma 1 (Invariance of semantic volume method under linear transformation). *Our method is invariant under linear transformation on the semantic volume measure $m(\cdot)$. More precisely, denote τ^* as the decision boundary defined in equation 4, we label*

$$y_i \stackrel{\text{def}}{=} \mathbf{1}_{m(s_i) < \tau^*}.$$

Given any linear transformation $T(m_i) \stackrel{\text{def}}{=} \alpha m_i + \beta$ ($\alpha > 0$) applied to the measure $m(\cdot)$, denote the new labels of our method under the new measure $T(m(\cdot))$ as

$$\tilde{y}_i \stackrel{\text{def}}{=} \mathbf{1}_{T(m(s_i)) < \tilde{\tau}^*}.$$

Then we have

$$\tilde{y}_i = y_i \quad \text{for all } s_i \in \mathcal{D} \setminus \mathcal{L}.$$

Proof. If we transform m_i to $\tilde{m}_i = T(m_i)$, the new threshold $\tilde{\tau}^*$ that maximizes the same metric still yields the same partition of the labeled samples. In other words,

$$m_i > \tau^* \iff T(m_i) = \tilde{m}_i > T(\tau^*),$$

a result of the simple fact that $m_i > \tau^* \iff \alpha(m_i) + \beta > \alpha(\tau^*) + \beta$. Thus our new threshold $\tilde{\tau}^*$ is effectively $T(\tau^*)$. Note that here if $\alpha < 0$ in $T(m_i) \stackrel{\text{def}}{=} \alpha m_i + \beta$, then naturally we should flip the decisions of our method and then the labels still remain the same. \square

Lemma 2 below provides the formula for differential entropy of Gaussian vectors. This is a known result but we include this lemma and provide a proof here for completeness.

Lemma 2 (Differential entropy of Gaussian vectors). *For $X \in \mathbb{R}^d$ that follows a multivariate normal distribution*

$$X \sim \mathcal{N}(\boldsymbol{\mu}, \boldsymbol{\Sigma}).$$

The differential entropy of X is given by

$$\mathcal{H}(X) = \frac{1}{2}(\log \det(\boldsymbol{\Sigma}) + d \log(2\pi) + d).$$

Proof. By the definition of the differential entropy and the probability density function of the multivariate normal distribution, we have

$$\begin{aligned} \mathcal{H}(X) &= - \int_X p(x) \log p(x) dx = -\mathbb{E}_{x \sim X} [\log p(x)] \\ &= -\mathbb{E} \log \left[\frac{1}{\sqrt{(2\pi)^d \det(\boldsymbol{\Sigma})}} \exp \left(-\frac{1}{2}(\mathbf{x} - \boldsymbol{\mu})^\top \boldsymbol{\Sigma}^{-1}(\mathbf{x} - \boldsymbol{\mu}) \right) \right] \\ &= \mathbb{E} \log \sqrt{(2\pi)^d \det(\boldsymbol{\Sigma})} + \mathbb{E} \left[\frac{1}{2}(\mathbf{x} - \boldsymbol{\mu})^\top \boldsymbol{\Sigma}^{-1}(\mathbf{x} - \boldsymbol{\mu}) \right] \\ &= \frac{1}{2} \mathbb{E} [d \log(2\pi) + \log \det(\boldsymbol{\Sigma})] + \frac{1}{2} \mathbb{E} [(\mathbf{x} - \boldsymbol{\mu})^\top \boldsymbol{\Sigma}^{-1}(\mathbf{x} - \boldsymbol{\mu})] \\ &= \frac{1}{2} (d \log(2\pi) + \log \det(\boldsymbol{\Sigma}) + \mathbb{E} [(\mathbf{x} - \boldsymbol{\mu})^\top \boldsymbol{\Sigma}^{-1}(\mathbf{x} - \boldsymbol{\mu})]) \end{aligned}$$

By the cyclic property of trace, we have

$$\begin{aligned} \mathbb{E} [(\mathbf{x} - \boldsymbol{\mu})^\top \boldsymbol{\Sigma}^{-1}(\mathbf{x} - \boldsymbol{\mu})] &= \mathbb{E} \text{Tr} [(\mathbf{x} - \boldsymbol{\mu})^\top \boldsymbol{\Sigma}^{-1}(\mathbf{x} - \boldsymbol{\mu})] \\ &= \mathbb{E} \text{Tr} [\boldsymbol{\Sigma}^{-1}(\mathbf{x} - \boldsymbol{\mu})(\mathbf{x} - \boldsymbol{\mu})^\top] \\ &= \text{Tr} \boldsymbol{\Sigma}^{-1} \mathbb{E} [(\mathbf{x} - \boldsymbol{\mu})(\mathbf{x} - \boldsymbol{\mu})^\top] \\ &= \text{Tr} \boldsymbol{\Sigma}^{-1} \boldsymbol{\Sigma} \\ &= d. \end{aligned}$$

Combine these steps, we get

$$\mathcal{H}(X) = \frac{1}{2}(\log \det(\boldsymbol{\Sigma}) + d \log(2\pi) + d).$$

\square

Lemma 3 (Eigenvalue distribution of rank-one perturbed matrix). *For matrix $\mathbf{M} \in \mathbb{R}^{d \times d}$ and any rank-one perturbation $\mathbf{S} \stackrel{\text{def}}{=} \mathbf{M} + \mathbf{u}\mathbf{v}^\top$, we have*

$$\log \det(\mathbf{S}) = \log \det(\mathbf{M}) + \log(1 - \mathbf{v}^\top \mathbf{M}^{-1} \mathbf{u}), \quad (5)$$

Proof. By the matrix determinant lemma [19], we have

$$\begin{aligned} \det(\mathbf{S}) &= \det(\mathbf{M} + \mathbf{u}\mathbf{v}^\top) = \det(\mathbf{M})(1 - \mathbf{v}^\top \mathbf{M}^{-1} \mathbf{u}) \\ \implies \log \det(\mathbf{S}) &= \log \det(\mathbf{M}) + \log(1 - \mathbf{v}^\top \mathbf{M}^{-1} \mathbf{u}). \end{aligned}$$

\square

Next, we combine the results above to derive the proof of Theorem 1.

Proof of Theorem 1. For each s (either a query or response) with embedding $\bar{\mathbf{x}} \in \mathbb{R}^d$, we extend it to get n perturbations $\mathbf{x}_1, \mathbf{x}_2, \dots, \mathbf{x}_n$. Equivalently, $\{\mathbf{v}_i\}_{i \in [n]}$ are perturbations of $\bar{\mathbf{v}}$. Assume the perturbation is Gaussian with covariance matrix Σ . Then $\{\mathbf{x}_i\}_{i \in [n]}$ are samples for a Gaussian vector $X \sim \mathcal{N}(\bar{\mathbf{x}}, \Sigma)$. Denote $\lambda_i(\mathbf{A})$ as the i -th largest eigenvalue of matrix \mathbf{A} . Note that $\mathbf{V}^\top \mathbf{V}$ and $\mathbf{V} \mathbf{V}^\top$ are both positive semi-definite matrices and share the same nonzero eigenvalues (can be easily proved using SVD of \mathbf{V}). Similarly for $\mathbf{X}^\top \mathbf{X}$ and $\mathbf{X} \mathbf{X}^\top$. We can diagonalize Σ as $\Sigma = Q \Lambda Q^\top$ where Q is an orthogonal matrix and $\Lambda = \text{diag}(\lambda_1, \dots, \lambda_d)$. Define an isotropic Gaussian vector $Z \sim \mathcal{N}(0, \mathbf{I}_d)$. Then we can write $X = Q \Lambda^{1/2} Z$. Hence we have

$$\mathbb{E}\|X\|^2 = \mathbb{E}[X^\top X] = \mathbb{E}[Z^\top \Lambda^{1/2} Q^\top Q \Lambda^{1/2} Z] = \mathbb{E}[Z^\top \Lambda Z] = \mathbb{E}\left[\sum_{i=1}^d \lambda_i Z_i^2\right] = \sum_{i=1}^d \lambda_i \mathbb{E}[Z_i^2] = \text{Tr}(\Sigma).$$

Note that in high-dimensions, $\|X\|^2$ is concentrated around its mean $\mathbb{E}\|X\|^2 = \text{Tr}(\Sigma)$ (particularly for isotropic Gaussian, this is \sqrt{D}). Under this regime, we have $\mathbf{V} \stackrel{\text{def}}{=} [\mathbf{v}_1, \mathbf{v}_2, \dots, \mathbf{v}_n] \approx \frac{1}{\sqrt{\text{Tr}(\Sigma)}} \mathbf{X}$.

Let $\alpha = n / \text{Tr}(\Sigma)$. Then

$$\log \det(\mathbf{V}^\top \mathbf{V}) \approx \log \det\left(\frac{1}{\text{Tr}(\Sigma)} \mathbf{X}^\top \mathbf{X}\right) = \log \det\left(\alpha \cdot \frac{1}{n} \mathbf{X}^\top \mathbf{X}\right) = \log \det\left(\frac{1}{n} \mathbf{X}^\top \mathbf{X}\right) + n \log \alpha. \quad (6)$$

Since our method sets a threshold τ^* on the log-determinant value, searched using a held-out set $\mathcal{L} \in \mathcal{D}$, the final classification is invariant to shifts (and more generally, to any linear transformation. See Proposition 1). Hence we can ignore the constant term $n \log \alpha$ and only focus on $\log \det\left(\frac{1}{n} \mathbf{X}^\top \mathbf{X}\right)$. We have

$$\log \det\left(\frac{1}{n} \mathbf{X}^\top \mathbf{X}\right) = \log \prod_{i=1}^n \lambda_i\left(\frac{1}{n} \mathbf{X}^\top \mathbf{X}\right) = \sum_{i=1}^n \log \lambda_i\left(\frac{1}{n} \mathbf{X}^\top \mathbf{X}\right) = \sum_{i=1}^n \log \lambda_i\left(\frac{1}{n} \mathbf{X} \mathbf{X}^\top\right).$$

Thus, it suffices to study the eigenvalues of $\frac{1}{n} \mathbf{X} \mathbf{X}^\top$. Note that we have

$$\begin{aligned} \mathbf{X} \mathbf{X}^\top - n \Sigma &= \left(\sum_{i=1}^n \mathbf{x}_i \mathbf{x}_i^\top\right) - \left(\sum_{i=1}^n (\mathbf{x}_i - \bar{\mathbf{x}})(\mathbf{x}_i - \bar{\mathbf{x}})^\top\right) \\ &= \sum_{i=1}^n (\bar{\mathbf{x}} \mathbf{x}_i^\top - \mathbf{x}_i \bar{\mathbf{x}}^\top + \bar{\mathbf{x}} \bar{\mathbf{x}}^\top) \\ &= \bar{\mathbf{x}} \left(\sum_{i=1}^n \mathbf{x}_i\right)^\top - \left(\sum_{i=1}^n \mathbf{x}_i\right) \bar{\mathbf{x}}^\top + n \bar{\mathbf{x}} \bar{\mathbf{x}}^\top \\ &\approx n \bar{\mathbf{x}} \bar{\mathbf{x}}^\top - n \bar{\mathbf{x}} \bar{\mathbf{x}}^\top + n \bar{\mathbf{x}} \bar{\mathbf{x}}^\top \\ &= n \bar{\mathbf{x}} \bar{\mathbf{x}}^\top. \end{aligned}$$

This implies that

$$\frac{1}{n} \mathbf{X} \mathbf{X}^\top - \Sigma \approx \bar{\mathbf{x}} \bar{\mathbf{x}}^\top. \quad (7)$$

Thus Σ is essentially a rank-one perturbation of $\frac{1}{n} \mathbf{X} \mathbf{X}^\top$. By Lemma 2, we know the differential entropy of X is:

$$\mathcal{H}(X) = \frac{1}{2} (\log \det(\Sigma) + d \log(2\pi) + d).$$

Again due to the invariance of our method to linear transformation, we can only focus on $\log \det(\Sigma)$. When d is large, by Lemma 3, let $\mathbf{M} \stackrel{\text{def}}{=} \frac{1}{n} \mathbf{X} \mathbf{X}^\top$, we have $\log \det(\Sigma) = \log \det \mathbf{M} + \log(1 + \bar{\mathbf{x}}^\top \mathbf{M}^{-1} \bar{\mathbf{x}}^\top)$. Note here $\bar{\mathbf{x}}$ is constant, and recall that \mathbf{M} concentrate around a deterministic matrix $\Sigma + \bar{\mathbf{x}} \bar{\mathbf{x}}^\top$ from equation 7 above (one can show $\|\mathbf{M} - (\Sigma + \bar{\mathbf{x}} \bar{\mathbf{x}}^\top)\| \xrightarrow{p} 0$ as $n \rightarrow \infty$, using standard random matrix theory tools). Therefore combining all above, we have derived that $\log \det \mathbf{M}$ is essentially shifted $\log \det(\Sigma)$ in high-dimensional regimes, and hence same for $\log \det \frac{1}{n} \mathbf{X}^\top \mathbf{X}$. This completes the proof. \square

D Numerical Stability with ϵ

Here, we present the distribution of the matrix norm $\|\mathbf{V}^\top \mathbf{V}\|$ (spectral norm) across our datasets in Figure 4. The histograms indicate that the chosen value of $\epsilon = 10^{-10}$ is negligible compared to the typical magnitude of $\|\mathbf{V}^\top \mathbf{V}\|$. This confirms that ϵ only serves to ensure numerical stability rather than influencing the quantification. Moreover, in practice, we observe that exact repetition among sampled perturbations is rare

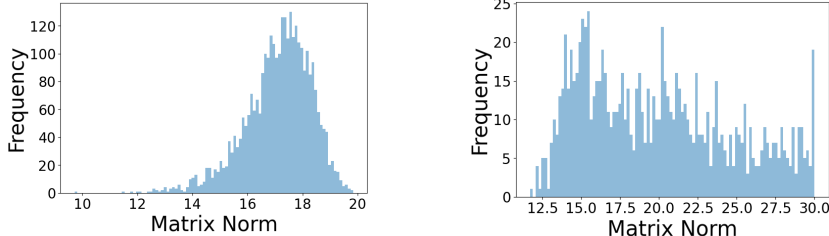


Figure 4: Distribution of the spectral norm $\|\mathbf{V}^\top \mathbf{V}\|$ for the perturbation embedding vectors (the left histogram corresponds to queries perturbations and the right is for response perturbations).

E Variation: Reduced Dimension d

In Figure 5, we illustrate the impact of varying d on performance. Additionally, we compare our method with the Semantic Volume that uses the original embedding vectors instead of the projected ones. Our results show that projecting to a lower-dimensional space improves performance, possibly because PCA projections better separate perturbation vectors. Furthermore, our study suggests that there may be an optimal, task-dependent choice of d . Exploring this further and characterizing the optimal d is left for future work.

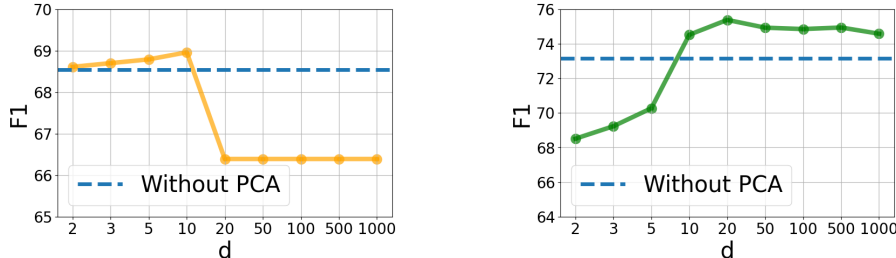


Figure 5: F1 scores for different dimension d in PCA dimension reduction. The dashed line represents the F1 score of the semantic volume method without dimension reduction. The left figure corresponds to the external uncertainty task, while the right figure corresponds to the internal uncertainty task.

F Variation: Perturbation Sample Size n

The perturbation sample size n is a hyperparameter in our method. A larger n provides a more comprehensive estimate of semantic dispersion but increases computational cost, while a smaller n may fail to capture sufficient variation, reducing the reliability of uncertainty quantification.

Figure 6 illustrates how varying n affects classification performance. In general, increasing n tends to improve F1 scores, likely due to a more accurate estimation of dispersion. However, beyond a certain point, the improvements diminish while the cost continues to rise. To balance efficiency and performance, we set $n = 20$ for external uncertainty detection and internal uncertainty detection.

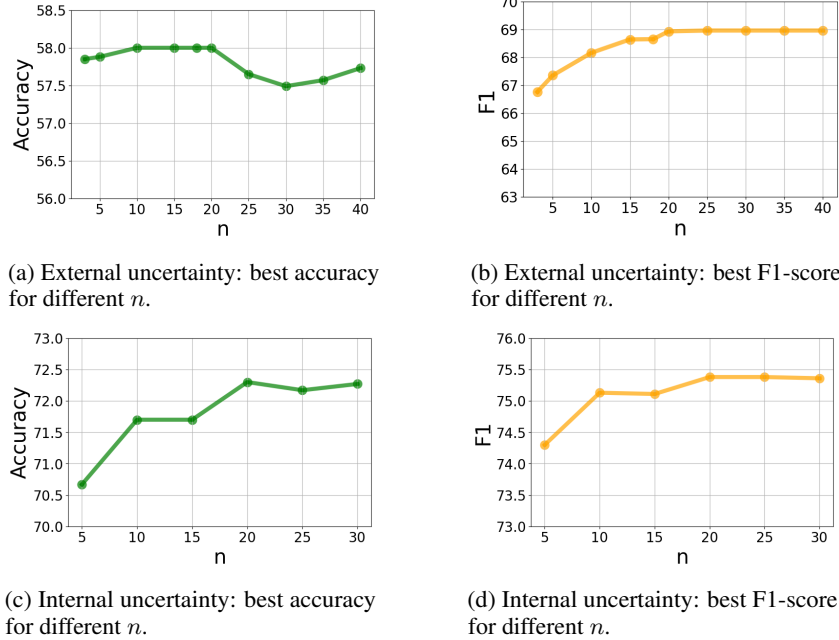


Figure 6

G Variation: Embedding Models

To examine the effect of different embedding models on our method, we explore two larger sentence-transformers: `Alibaba-NLP/gte-Qwen2-7B-instruct` (embedding dimension 3584) from the same Qwen family as used in our main results, and `nvidia/NV-Embed-v2` (embedding dimension 4096) from a different model family. Using the external uncertainty task as a case study, we present the results in Table 4. Our findings indicate that models from different families but with similar sizes produce comparable results. Compared to the Qwen-1.5B sentence transformer used in the main results, performance remains largely similar—while the 7B model achieves slightly higher accuracy but lower F1 score, this difference may not be statistically significant.

	Qwen2-7B		NV-Embed	
	Accuracy	F1	Accuracy	F1
$n = 25$	57.8	68.0	57.4	67.5
$n = 20$	58.1	68.0	58.4	67.9
$n = 15$	57.7	68.1	57.9	67.8
$n = 10$	57.2	67.7	57.4	67.5
$n = 5$	56.8	66.9	57.7	67.0

Table 4: Performance with different embedding models.

H Variation: Response Generation Model

To assess the generalizability of our method, we repeat the experiment for internal uncertainty detection but replaced `Llama3.2-1B` with `LLama3.8B`, a larger LLM. Notably, with a larger model, the probability-based methods show higher latency. In our experiment, both Last Token Entropy and Log Probabilities took more than 4 hours on a H100-80GB GPU. Furthermore, similar to Table 2, we observe that methods relying on prompting the LLM (including `pTrue`) sometimes exhibit a strong bias toward predicting almost exclusively “Yes” or “No”. In Table 5, for example, *Prompt Llama3.2-1B* and *pTrue (Llama3.2-1B)* predict nearly all samples as “Yes”, whereas *pTrue (Mistral*

7B) predicts almost all as “No”. This instability highlights another drawback of using prompted LLMs for uncertainty prediction.

Method	Accuracy	F1
Prompt Llama3.2-1B	50.1	66.5
Prompt Llama3-8B	65.5	64.0
Prompt Mistral-7B	60.4	54.3
Last Token Entropy	56.2	55.9
Log Probabilities	53.4	51.1
pTrue (Llama3.2-1B)	50.0	66.6
pTrue (Llama3-8B)	55.2	23.2
pTrue (Mistral-7B)	50.8	4.3
Lexical Similarity	64.2	72.0
Semantic Entropy	63.5	69.4
Semantic Volume (ours)	72.0	74.9

Table 5: Internal Uncertainty: Performance comparison based on Accuracy and F1 score.

Method	AUROC
Last Token Entropy	63.9
Log Probabilities	54.4
pTrue (Llama3.2-1B)	55.1
pTrue (Llama3-8B)	52.8
pTrue (Mistral-7B)	72.7
Lexical Similarity	78.7
SemanticEntropy	73.2
Semantic Volume (ours)	79.7

Table 6: Internal Uncertainty: Performance comparison based on AUROC.

I Hallucination Detection Pipeline using both External and Internal Uncertainty

In this paper, we conducted separate experiments on external uncertainty detection and internal uncertainty detection to demonstrate that the Semantic Volume is an effective method that can be generally applied to both tasks. In practice, these two tasks can be combined into a unified pipeline for hallucination detection (see Figure 7): First, we perform the internal uncertainty detection. If high uncertainty is detected in the response, then hallucination is likely to happen. Then at the second step, we check the external uncertainty: If the query is detected to be ambiguous, the LLM should ask a clarification question to the user. After clarification is provided or additional information is provided to resolve the ambiguity in the query, the LLM can then generate the answer to the query. On the other hand, if external uncertainty is ruled out, then the hallucination is likely caused by internal lack of knowledge of the LLM. This can be addressed through various methods such as retrieval-augmented generation (RAG), reasoning-based approaches, or by leveraging stronger LLMs or human agents.

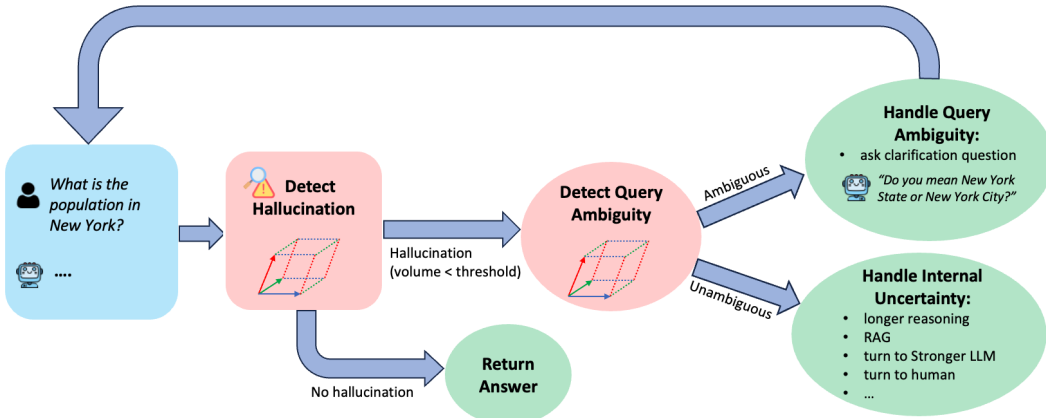


Figure 7: Complete pipeline for hallucination detection utilizing both external and internal uncertainty.

Moreover, all of our experiments are set up as classification tasks for uncertainty detection, relying on a threshold-based decision. However, these uncertainty measures can also be applied to comparison or ranking tasks.

J Prompts

J.1 Prompt template to extend queries.

Provide a paraphrase of the following question with a contextual expansion, while maintaining its core meaning. The filled context information should be diverse but must be concrete and specific (it cannot be a placeholder or a template). Only reply with the new version of the question and nothing else.

Question:

{question}

J.2 Prompt template for query ambiguity detection

Is the following question ambiguous? A question is ambiguous if it can be interpreted in multiple ways or has multiple possible answers. If the question is ambiguous, then reply ‘Yes’, otherwise reply ‘No’. Only reply with ‘Yes’ or ‘No’ and nothing else.

Question:

{question}